



The effect of hydrogenation on the fracture of Ti₂AlNb-based alloy during ball milling



K.S. Senkevich^{a,*}, O.Z. Pozhoga^a, E.A. Kudryavtsev^b, V.V. Zasyplin^a

^a *Moscow Aviation Institute (National Research University), 125993 Moscow, Russia*

^b *National Research University "Belgorod State University", 308015 Belgorod, Russia*

ARTICLE INFO

Article history:

Received 12 September 2021

Received in revised form 11 January 2022

Accepted 13 January 2022

Available online 15 January 2022

Keywords:

Ti₂AlNb orthorhombic alloys

Ball milling

Rapid solidification

Intermetallic hydride

HDH-powders

ABSTRACT

In this work we have studied the effect of phase composition and microstructure of a rapidly solidified Ti₂AlNb-based alloy containing hydrogen on deformation of the alloy during ball milling and production of a fine-dispersed powder. Hydrogen is introduced into the alloy up to a concentration of 2.0 wt%. The X-Ray diffraction (XRD) analysis and Scanning Electron Microscopy (SEM) show that the alloy has the following phase compositions depending on hydrogen content: β + O, β/β-hydride, β/β-hydride + intermetallic hydride (Ti₂AlNbH_x) or a single-phase intermetallic hydride. It is found that in the hydrogenated β + O alloy containing a small amount of hydrogen a strong decrease in ductility occurs, but this does not affect the ball milling and synthesis of the fine-dispersed powder. Efficient milling of the rapidly solidified alloy has been achieved when hydrogen content was 1.2 wt% and exceeding this value when a transformation from the H-saturated solid solution into a hydride phase is observed in the alloy or the formation of a single phase hydride occurs.

© 2022 Elsevier B.V. All rights reserved.

1. Introduction

Orthorhombic titanium aluminides are advanced aerospace materials for use at temperatures above 550 °C when high temperature titanium alloys can no longer work due to their low heat resistance, and titanium gamma aluminides have low fracture toughness and cracking resistance. Also, orthorhombic alloys have an advantage over nickel alloys and heat-resistant steels that are currently widely used at these temperatures due to their lower density [1,2]. To obtain Ti₂AlNb-based alloys, various powder metallurgy and additive manufacturing methods are being actively explored in addition to conventional foundry metallurgy, thus making it possible to eliminate typical foundry problems, i.e., chemical inhomogeneity and areas with variable densities and microstructure in ingots. These methods are valued for a high material utilization rate and the possibility of synthesizing semi-finished products with near-net shape or complex geometries using additive technologies. Atomized alloyed powders [3–5] or blended elemental powders [6–8] are used as raw materials for the production of orthorhombic titanium aluminides. Both approaches have disadvantages. For example, pre-alloyed powders are produced by labor-consuming and expensive

methods of atomizing or melt atomization. They also have smooth spherical surface and are not capable of mechanical adhesion during cold compaction at room temperature. Therefore, their application in the simplest powder metallurgy methods, i.e., cold compaction and pressureless sintering (CC and PS), is difficult or only becomes possible if one uses binders which can lead to alloy contamination by impurities.

The use of non-spherical blended elemental powders or mixtures of non-spherical and spherical powders allows production of sintered orthorhombic titanium aluminides by the CC and PS methods as well as by hot compaction or additive manufacturing. However, chemically unbound refractory niobium in the powder mixture requires high temperatures and diffusion dissolution or homogenization of sintered alloys. This complicates the technology of sintered orthorhombic titanium aluminides. Using non-spherical pre-alloyed powders would make the CC and PS methods simpler and economically advantageous.

Non-spherical powders of titanium and its alloys synthesized by the hydrogenation-dehydrogenation (HDH) method are being more and more widely used nowadays. This method was developed in 1957 by the Titanium Metals Corporation and is mainly employed for the production of low-cost powders from commercially pure titanium (CP-Ti) [9], less often from the Ti-6Al-4V alloy [10]. These powders exhibit a good compactibility, are readily sintered and have already found practical application in the manufacturing of titanium

* Corresponding author.

E-mail address: senkevichks@yandex.ru (K.S. Senkevich).

products for the automotive and aerospace industries at Dynamet Technology, USA, using the technology of cold isostatic pressing and sintering [11]. It is also possible to use titanium hydride powders subjected to cold compaction and subsequent dehydrogenation during sintering [12,13]. This method is used for aerospace, automotive and medical applications by ADMA Products, Inc. [12,14].

The HDH method has already been experimentally tested for the production of powders from intermetallic and high-entropy alloys such as TaNbHfZrTi, Nb-Mo-Si, and Nb-20% Ta [15–17], but its application for the synthesis of pre-alloyed powders from titanium aluminides has not yet been studied. This method can also be very attractive for the fabrication of non-spherical pre-alloyed powders from orthorhombic titanium aluminides and the production of sintered alloys based on the Ti_2AlNb compound using cold compaction and pressureless sintering technology.

The HDH method is quite simple and involves hydrogenation of the required material, milling and subsequent dehydrogenation and deagglomeration of the dehydrogenated powder. It is applied to materials that readily adsorb hydrogen. This method has been well studied for the industrial production of powders from titanium; however, its application for powders of orthorhombic titanium aluminides requires a detailed study of all the stages of HDH-powder synthesis. The hydrogenation stage is very important for determining the optimum concentration of hydrogen which converts the material to a brittle hydrogenated state when it can be easily milled to a dispersed state. In this case, excessive hydrogen can make the material excessively brittle, and then an undesirable dust-like powder will form during milling. However if the amount of hydrogen is not excessive, the material becomes only slightly brittle, and its processing will require a longer processing time during the ball milling or a higher energy of the milling bodies. It is of great importance to take into account that the hydrogenation of a material to high hydrogen concentrations is technically difficult, and it is critical to find the optimum amount of hydrogen at which the material is highly brittle and which can be easily absorbed under industrial conditions. For example, as pure titanium is capable of absorbing up to 4.0 wt% of hydrogen, the optimum hydrogen concentration for hydrogenation and milling should not exceed 3.5 wt% H [9].

We earlier proved the possibility of producing powders from the VTI-4 (trademark) alloy based on the Ti_2AlNb compound by milling of rapidly solidified fiber fabricated by the pendent drop melt extraction (PDME) method and hydrogenated to 0.88 wt% H [18]. The size of the milled particles was large enough, 10–80 μm , and discrete fiber fragments were also observed. We explained this by the small amount of hydrogen in the alloy which does not cause its heavy embrittlement. To determine the optimum concentration of hydrogen which converts the Ti_2AlNb -based alloy to a brittle state and provides efficient milling, it is required to study how variable hydrogen content affects the deformation of orthorhombic titanium aluminide during the ball milling. Since orthorhombic titanium aluminide may have different phase compositions, the effect of hydrogen on the phase composition of the alloy should be analyzed.

The aim of this work is to study the effect of the phase composition and microstructure of the rapidly solidified Ti_2AlNb -based alloy with various hydrogen contents on the deformation of the alloy during ball milling and the production of fine-dispersed powders. The results will be analyzed with the aim to determine the optimum hydrogen concentration and the phase composition of the Ti_2AlNb -based alloy which provide for efficient ball milling.

2. Experimental procedures

The studies were carried out for the commercial VTI-4 titanium alloy (based on the Ti_2AlNb compound) which contains a two-phase β (body centered cubic lattice) + O (orthorhombic lattice)

composition. The alloy was obtained by vacuum-arc melting and had the following composition: Ti-12.0Al-41.2 Nb-0.89Mo-0.83 V-1.27Zr-0.13Si, wt%. Rapidly solidified fiber was fabricated using the PDME method by vacuum melting of an as-cast alloy electrode with electron-beam melting equipment (Fig. 1a) [19]. Since the as-cast alloy is hydrogenated only after a long-term exposure to hydrogen and can hardly absorb more than 0.5 wt% H at a pressure of about 0.1 MPa regardless of phase composition (β or O phase) [20], the study was carried out for the rapidly solidified alloy. Hydrogenation was carried out using the Sieverts method in an installation with a hydrogen atmosphere containing up to 0.2 – 2.0%¹ H at 800 °C in accordance with the following technique: vacuum heating of the alloy fiber to 800 °C and exposure to a constant temperature; hydrogen charging during exposure for 10 min for achieving a uniform hydrogen distribution over a thin fiber section; and cooling to room temperature. The installation consisted of a vacuum system, a hydrogen source (titanium hydride), a system for hydrogen purification from gaseous impurities, a gas cylinder in which a predetermined hydrogen pressure was developed by controlled hydrogen charging and a pre-evacuated retort with the hydrogenated material where its hydrogenation occurs. The amount of hydrogen introduced into the chamber of the installation was determined on the basis of the pressure change in the pressure in the closed vacuum system with a known volume and evaluated based on the weight gain of the samples using an Adventure AR2140 electronic laboratory balance with an absolute measurement error of within 0.0001 g. Ball milling was conducted in a planetary-type ball mill for 5–20 min in alcohol at a 100 rpm rate. XRD analysis of the phase composition of the rapidly solidified alloy in the initial and hydrogenated states was carried out using a DRON-7 diffractometer (Russia) using $CuK\alpha$ radiation at 40 kV and 20 mA. The microstructure of the alloy and the fractures of the hydrogenated fiber and the milled powders were observed using a field emission-scanning electron microscope (FE-SEM) (FEI, QUANTA FEG 250) equipped with an energy-dispersive spectrometer (EDS) (EDAX, Octane Elite EDS) and under a JEM-2100 analytical electron microscope. The microhardness was measured using a MicroMet 5101 hardness tester with a diamond pyramid at a load of 0.5 N, and the average values were calculated.

3. Results and discussion

3.1. Phase composition and microstructure of the hydrogenated alloy

Rapid solidification of orthorhombic titanium aluminides by PDME or powder atomization leads to the formation of the metastable β phase (Fig. 1b) [20–22]. We earlier studied [23] the phase composition of the quenched cast VTI-4 alloy in the hydrogenated state and plotted the phase diagram for the VTI-4 alloy vs H content. The study showed that at 800 °C (the hydrogenation temperature) the alloy containing 0.1–0.3% H had a two-phase β + O composition. XRD study of the rapidly solidified alloy showed that after hydrogenation of the alloy containing 0.2% H only the peaks of the initial β -phase were observed (Fig. 2, a), and the lattice parameter changed slightly from 0.326 nm (the initial non-hydrogenated rapidly solidified alloy) to 0.329 nm (0.2% H). SEM analysis revealed fine-lamellar precipitates in the alloy (Fig. 2b) indicating a partial decomposition of the β -phase due to the hydrogenation and precipitation of the orthorhombic phase particles which were not detected by XRD analysis due to the small content of the precipitates. Transmission electron microscopy (TEM) showed that the lamellar precipitates are the orthorhombic phase (Fig. 2a). The small number of the orthorhombic phase precipitates is associated with the higher thermal stability of the metastable β -phase forming due to rapid

¹ Hereinafter, the content of hydrogen is given in wt%.

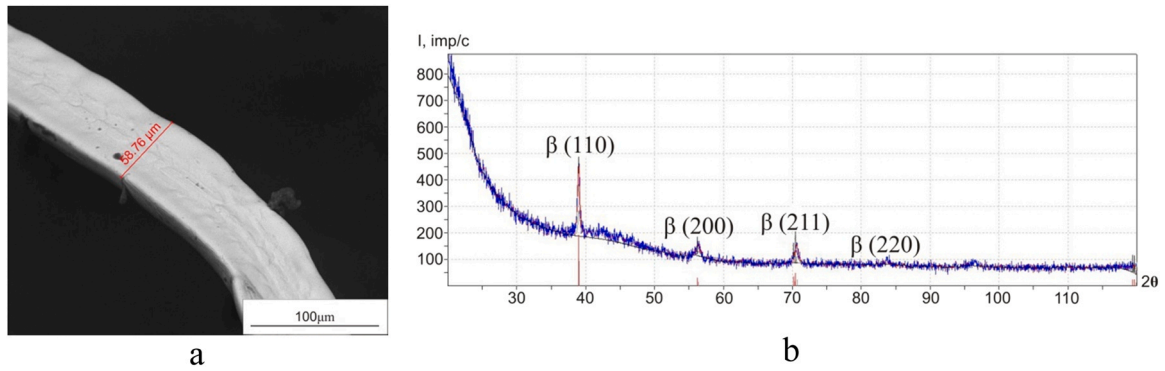


Fig. 1. Rapidly solidified Ti_2AlNb -based alloy: (a) the fiber and (b) XRD pattern.

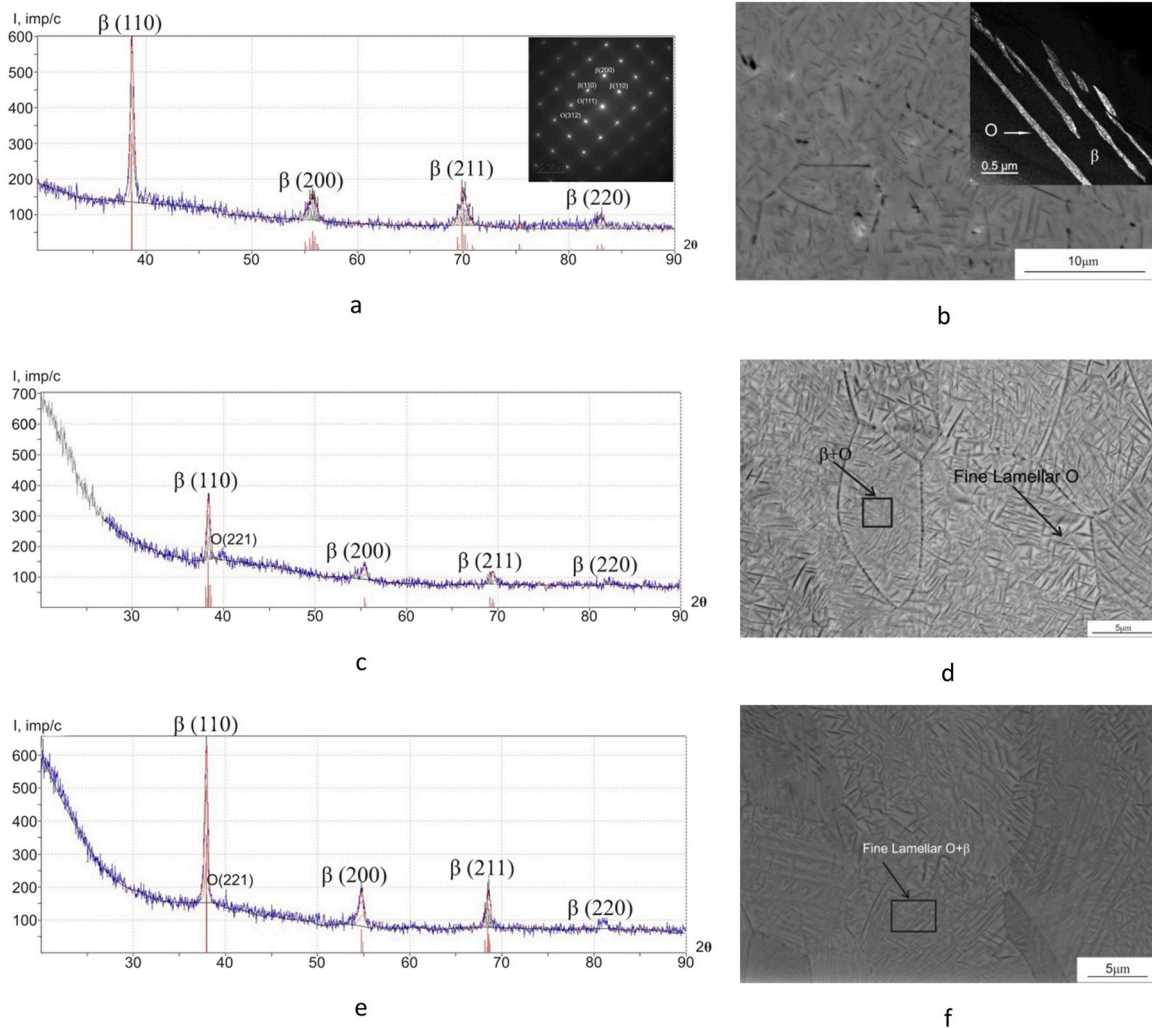


Fig. 2. (a, c, e) XRD patterns, (a) inset: TEM diffraction pattern, and (b, d, f) microstructures of the rapidly solidified Ti_2AlNb -based alloy after hydrogenation, wt% H: (a and b) 0.2; (c and d) 0.5; (e and f) 1.0.

solidification. We showed using DSC analysis [20] that heating of the rapidly solidified alloy to 1200 °C does not produce thermal peak of β phase decomposition at low temperatures (below 900 °C). We also do not observe the peak of subsequent high-temperature $\text{O} \rightarrow \beta$ transition at about 1000–1100 °C. Partial $\beta \rightarrow \text{O}$ decomposition and $\text{O} \rightarrow \beta$ transition are observed in quenched cast alloy for the same heating mode.

In addition, the phase diagram for the VTI-4 alloy vs H content was plotted for quenching of the hydrogenated cast alloy from

various temperatures after a long-term homogenization when an equilibrium phase composition was formed. Therefore, this diagram cannot be used to adequately predict the phase composition of the rapidly solidified alloy hydrogenated by short-term exposure.

Hydrogenation yielding 0.5% H leads to the precipitation of a greater number of O phase particles which are clearly observed in the XRD patterns; thus the alloy has a two-phase $\beta + \text{O}$ composition (Fig. 2c and d). The same tendency can be observed after hydrogenation until 0.65% and 1.0% H (Fig. 2e and f): the number of the O

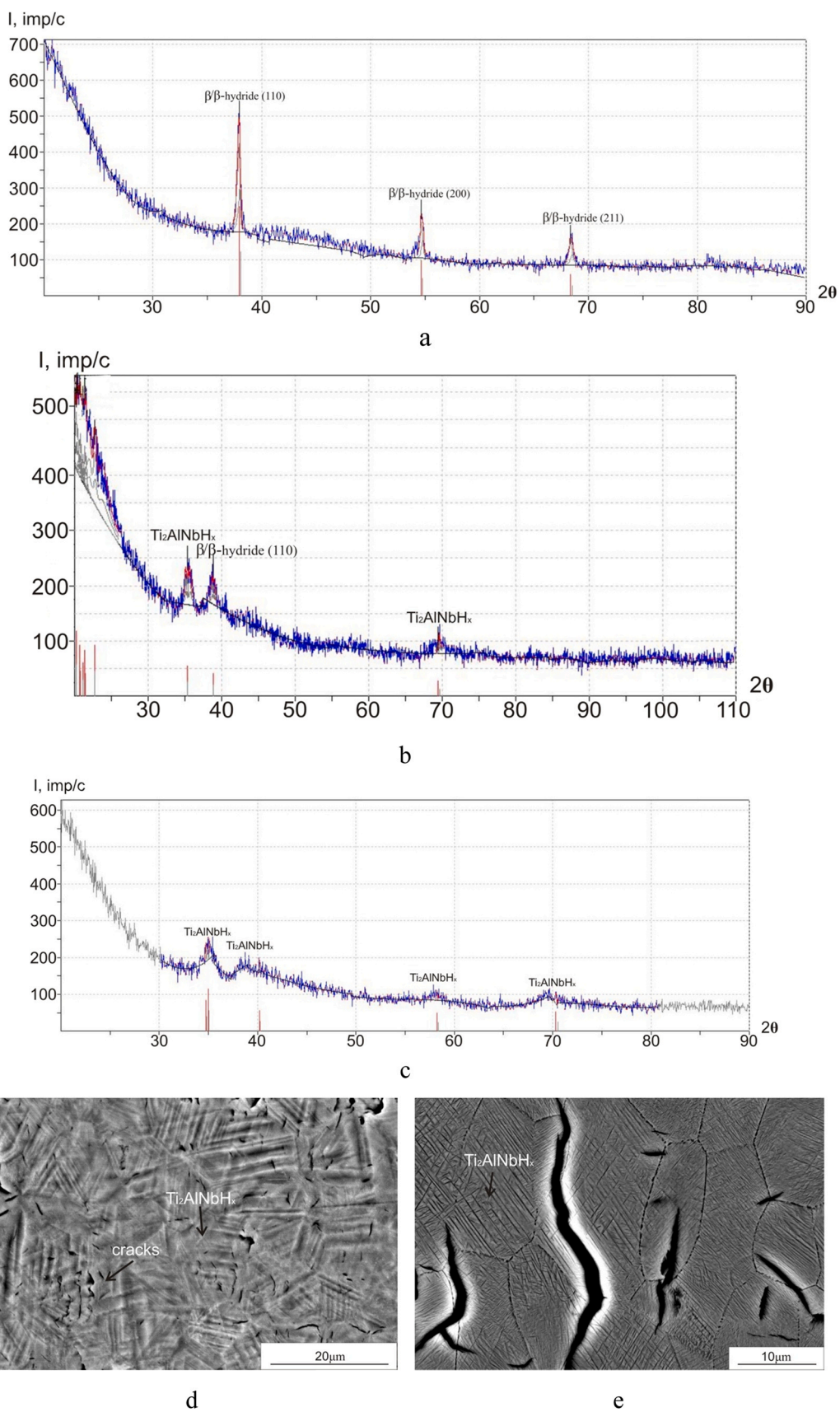


Fig. 3. (a, b, c) XRD patterns and (d, e) microstructures of the rapidly solidified Ti₂AlNb-based alloy after hydrogenation, wt% H: (a) 1.2; (b and d) 1.7; (c and e) 2.0.

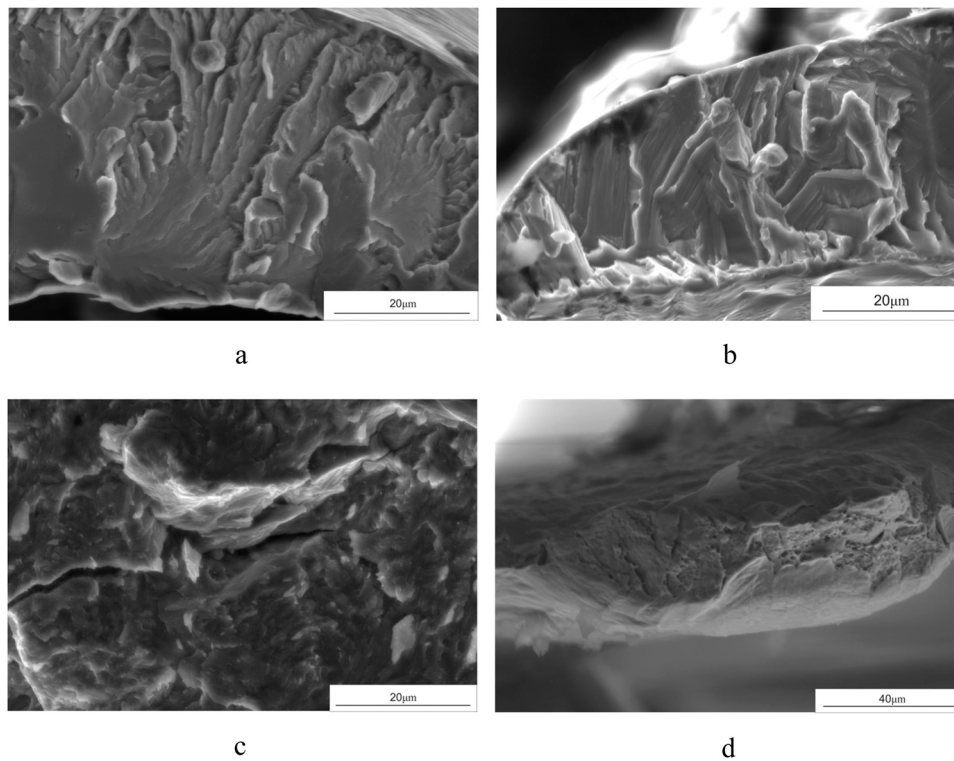


Fig. 4. (a, b, c) Fracture surface of fiber fragments and (d) fiber destroyed under a tensile load for the hydrogenated alloy, wt% H: (a) 0.5; (b) 0.65; (c) 1.7; (d) 0.2.

phase particles increases and the β phase lattice parameter grows gradually from 0.332 nm (0.5% H) to 0.335 nm (1.0% H).

Alloy hydrogenation providing a concentration of 1.2% H results in the formation of a single-phase solution. There are no O phase peaks in the XRD pattern (Fig. 3a), only the β phase being observed and its lattice parameter not changing in comparison with that for the alloy containing 1.0% H, which can indicate a limited solubility of hydrogen in the β phase. The disappearance of the orthorhombic phase peak may be due to its transformation into the so-called β -hydride undergoing anisotropic lattice rearrangement as observed earlier [24]. It was shown that during hydrogenation of the two-phase β +O orthorhombic titanium aluminide the β and O phases readily absorbed hydrogen, and at a hydrogen/metal ratio of 0.6 which corresponds to a hydrogen content of about 1.1%, β -hydride formed in the alloy, but a weak peak of the hydrogenated O phase still persisted which we also observed in our rapidly solidified alloy hydrogenated with 1.0% H. However the authors showed [24] that the β phase \rightarrow β -hydride phase transformation occurs due to isotropic deformation (expansion) of the β phase lattice, and β -hydride retains the bcc lattice inherited from the β phase. In our opinion the gradual increase of the β phase lattice parameter from 0.326 nm (initial state) to 0.332 nm (1.2% H) which we observed indicates the high ability of the β phase to absorb hydrogen rather than the formation of highly alloyed β -hydride. However, analysis of the Ti_2AlNb crystal structure alloyed with a large number of elements and saturated with a high concentration of hydrogen is a separate complex problem which is beyond the scope of this study. One can assume that the absence of the O phase peaks and the presence of the initial highly hydrogenated β phase in the alloy can indicate its transformation to a β -hydride. Hereinafter we will indicate this phase as β/β -hydride.

Hydrogenation of the alloy yielding a concentration of 1.4–1.7% H leads to the formation of a two-phase composition: the highly hydrogenated β/β -hydride and a new precipitated phase, i.e., an intermetallic hydride ($\text{Ti}_2\text{AlNbH}_x$) (Fig. 3b). At a high hydrogen/metal

ratio the formation of γ -hydride should occur in unalloyed orthorhombic titanium aluminide, while the presence of the orthorhombic phase facilitates the β -hydride (bcc) \rightarrow γ -hydride (bct) transformation [24]. Hydrogen ordering in the O phase is required in order to reduce the lattice mismatch between the O and β phases and facilitate the nucleation of the γ -hydride phase at the O/ β interfaces [25]. XRD analysis of the high alloyed intermetallic orthorhombic Ti_2AlNb -based alloy hydrogenated up to 1.4–1.7% H did not allow us to reliably identify the forming hydride ($\text{Ti}_2\text{AlNbH}_x$) as γ -hydride. Perhaps this is due to the fact that the ordering of hydrogen atoms in the O phase and β -hydride lattices of our alloy is accompanied by a redistribution of alloying elements that affects the β -hydride \rightarrow γ -hydride transformation. However, it can be stated that the new phase is indeed a hydride due to the difference between its peaks in the diffraction pattern, the reflection angles which are typical of the β phase and a higher hydrogen/metal ratio than that for β/β -hydride (Fig. 3b).

A fine-grained structure with a large number of thin hydride plates is observed in the microstructure of the alloy containing 1.4–1.7% H (Fig. 3d). Hydrogenation to reach 2.0% H results in the formation of a single-phase intermetallic hydride ($\text{Ti}_2\text{AlNbH}_x$) (Fig. 3c).

Microstructure analysis of the fiber hydrogenated with 0.2–2.0% H did not reveal any changes in the grain size with an increase in hydrogen content; no cracks or pores were observed in fibers with a hydrogen content of 1.2% or lower. There are only few cracks in the alloy containing 1.5% H. The microstructure of the alloy hydrogenated up to 1.7–2.0% H contains numerous cracks. Cracking occurs inside the grains and at the grain boundaries, the distance between the cracks being less than 15 μm (Fig. 3d and e). This indicates that the precipitation of the hydride phase in the alloy induces high internal stresses which lead to the initiation of cracks inside the fiber and on its surface. Unfortunately, it is difficult to establish a relation between the volume fraction of the hydride phase in the alloy and the concentration of introduced hydrogen due to a difficulty of differentiation between the β phase and β -hydride.

3.2. Analysis of brittleness and hardness of the hydrogenated alloy

After hydrogenation of the alloy for H content 0.5% or higher, its strong embrittlement is observed. Compacted elastic fiber placed into a steel container before hydrogenation undergoes disintegration after the hydrogenation under slight pressing (0.5% H) or transforms into a pile of separate fragments (0.65% H or higher). The cause is the hydrogen-induced brittleness of the alloy related to the various mechanisms of hydrogen interaction with the alloy: hydrogen restriction of dislocation mobility, initiation of intergranular fracture or decohesion at the matrix-hydride interface in the case of hydride particles precipitation [26,27]. This develops internal stresses in the alloy and leads to its brittle failure, which is indicated by pronounced brittle fracture of fiber fragments in the steel container after hydrogenation of 0.5% H or higher. The fragments have almost flat fracture surfaces and a large number of cleavage surfaces (Fig. 4a, b and c). Deep internal cracks can also be seen in the fracture images of the fiber fragments for 1.7% H (Fig. 4c). Fiber containing 0.2% H retains certain strength and ductility and can only be destroyed under a tensile load; plastic fine-grained fracture is then observed (Fig. 4d).

Fractographic analysis of hydrogenated fiber fragments showed that despite the absence of cracks and micropores in the microstructure of the alloy containing 0.5–1.2% H (Fig. 2d and f) it demonstrates a sharp decrease in the ductility by analogy with the alloy containing 1.5–2.0% H.

The PDME method shows a high hardness of the rapidly solidified Ti_2AlNb alloy which exceeds that of the deformed (hot-rolled) alloy: 516 and 467 HV, respectively [28]. This is associated with the formation of the single β phase with a high density of crystal structure defects formed in the metastable rapidly solidified state. Vacuum annealing of the rapidly solidified Ti_2AlNb alloy favors a decrease in the microhardness due to stress relaxation in the β phase [28] and partial precipitation of the O phase [18].

Study of the microhardness of the hydrogenated alloy showed a great influence of hydrogen content and phase composition on the alloy hardness (Fig. 5). At 0.2% H the two-phase $\beta + O$ alloy with a small amount of fine-dispersed lamellar O phase has an average hardness of 312.5 HV. A sharp decrease in the hardness of the rapidly solidified alloy is affected by several processes: stress relaxation during heating and holding as well as partial decomposition of the β phase during the hydrogenation and precipitation of O phase particles.

An increase in the amount of hydrogen to 0.5% and in the content of the O phase plates results in a slight growth of the hardness to 356.3 HV. Hydrogenation up to 0.65% and 1.0% H raises the hardness to 403 HV and 435 HV, respectively. A sharp increase in the microhardness (to 480 HV) is observed at 1.2% H when a single-phase β/β -hydride structure forms, which may indeed indicate the hydride

nature of the highly hydrogenated β phase. Further increase in the hydrogen content and the precipitation of an intermetallic hydride or the formation of a single-phase composition (Ti_2AlNbH_x) also dramatically increase the hardness of the alloy to above 700 HV.

A gradual increase in the hardness of the alloy containing 0.2 – 1.0% H and its subsequent two-stage rapid growth caused by hydrogenation with 1.0 – 1.2% H and 1.2 – 1.5% H (Fig. 5) are associated with a change in the phase composition of the alloy from the two-phase $\beta + O$ one to the hydride phase, which is in agreement with the XRD data.

At a hydrogen concentration of 1.5–2.0% the test alloy is no longer an orthorhombic titanium intermetallic compound but a highly alloyed intermetallic hydride, and the experimentally measured distinctly high hardness is a physical property which is more typical of this compound rather than of a hydrogenated orthorhombic titanium intermetallide.

The experimental microhardness data account for the brittle fracture of the alloy after hydrogenation. The high hydrogen content in the alloy (0.65–1.0%) favors the formation of a highly hydrogenated β/β -hydride and a large increase in the hardness. The hydrogenation to 1.4–2.0% H leads to the formation of a chemical compound, i.e., an intermetallic hydride, which does not show any significant ductility.

3.3. Study of hydrogenated alloy fracture under ball milling

In this work we studied the susceptibility of orthorhombic titanium aluminide to deformation during ball milling which is promoted by hydrogen embrittlement. Usually, studies of the effect of hydrogen embrittlement on the mechanical properties of metals include determining the maximum permissible hydrogen concentrations at which no noticeable degradation in strength and plasticity occurs. For this reason, the mechanical properties of metals and alloys containing different amounts of hydrogen are determined using mechanical tests. The aim of our work is opposite, i.e., to determine the hydrogen concentration at which a catastrophic decrease in the strength and plasticity of the hydrogenated alloy occurs, which makes it possible to mill the alloy into the smallest possible fragments, i.e., fine-dispersed powders. We therefore applied a treatment in a planetary ball mill not only as a method of producing powders but also as a method of studying disintegration of the alloy under multiple shock and shear loads during ball milling.

The degree of milling of hydrogenated titanium powders depends on the rate and time of milling and is not affected by the protective milling medium used (air, argon, alcohol, etc.); therefore in our experiment we used the simplest milling method, i.e., milling in alcohol.

It was found that ball milling of the fiber containing 0.2% and 0.5% H does not allow one to obtain powder. Milling results in the formation of large fiber fragments due to the absence of hydride particle precipitation in the alloy at this low hydrogen content, with the alloy still retaining certain strength and ductility.

After milling of the fiber containing 0.65% H for 20 min, a mixture of large particles (more than 100 μm in size) and discrete long fiber fragments was obtained (Fig. 6a). A sharp decrease in the size of the fragments was observed after milling of the fiber containing 1.0% H. After milling for 5 min most of the particles had a size of less than 100 μm and differed greatly in width, length and thickness. Furthermore, discrete long fibers and small fiber fragments were observed in the resultant mixture. Several particles less than 100 μm in size and a large number of round-shaped particles with sharp edges or flattened particles less than 70 μm in size were observed after milling for 20 min (Fig. 6b). The dispersion of the milled particles increased if hydrogen content grew to 1.2%, while the milling time strongly affected the sizes of the particles. After milling for 5 min

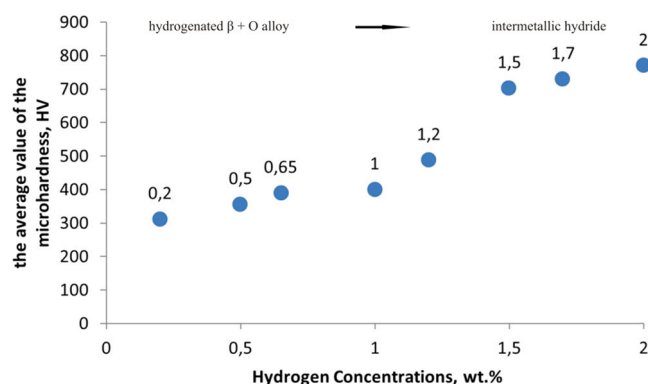


Fig. 5. Alloy microhardness vs hydrogen concentrations.

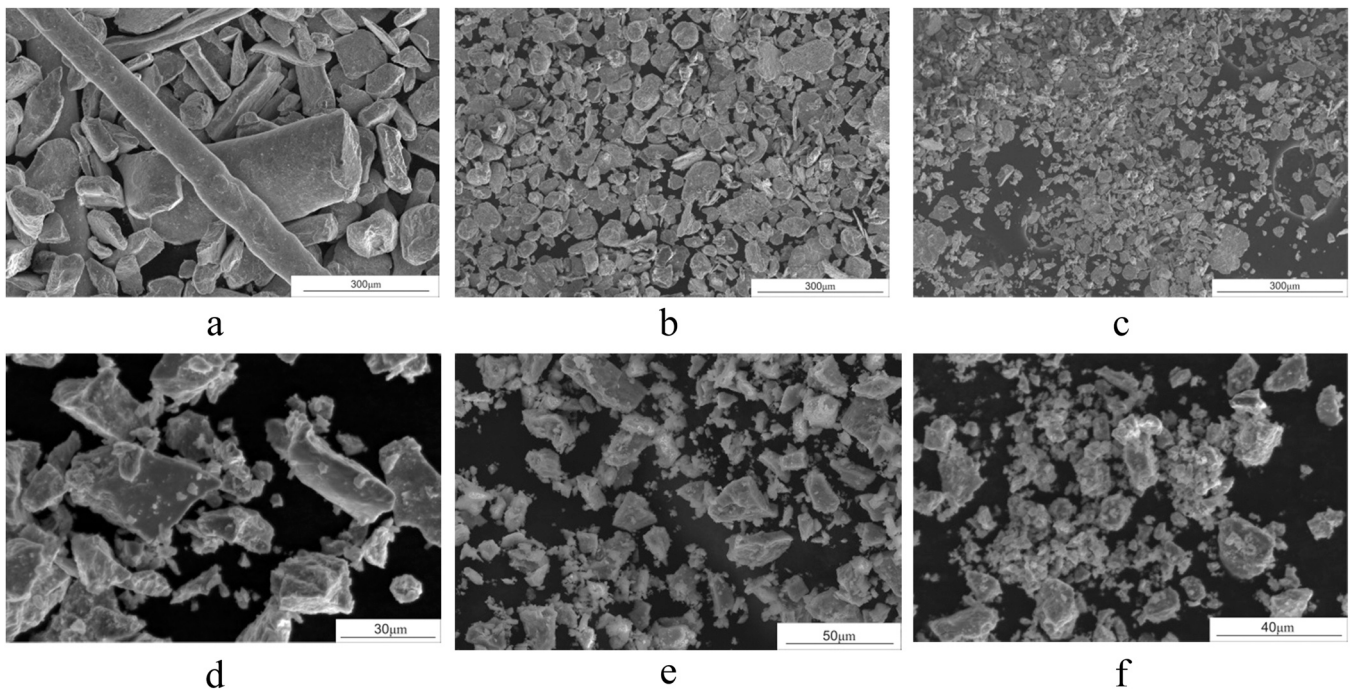


Fig. 6. Ball-milled powders of the Ti_2AlNb -based alloy after 20 min milling: (a) 0.65% H; (b) 1.0% H; (c) 1.2% H; 10 min: (d) 1.5% H; 5 min: (e) 1.7% H; (f) 2.0% H.

coarse particles or fragments distinguishing the fiber contours were still observed, and after milling for 20 min a mixture of particles less than $50\ \mu m$ in size and a small number of particles less than $30\ \mu m$ in size formed (Fig. 6c).

The alloy containing 1.5% H or higher has a very high brittleness which favors efficient milling of the fiber and synthesis a fine-dispersed powder. Milling of the fiber containing 1.5% H for 5 min produced powder with particles of less than $30\ \mu m$ in size and a large number of $1\text{--}5\ \mu m$ particles (Fig. 6d). An increase in the milling time did not affect the particles size. A similar result was obtained after ball milling of fiber containing 1.7% and 2.0% H. 5-min. ball milling provided for a high milling quality and produced dispersed powder less than $30\ \mu m$ in size: discrete $10\text{--}30\ \mu m$ particles and numerous small $1\text{--}20\ \mu m$ particles were observed (Fig. 6e and f).

4. Discussion

The experimental results for milling of hydrogenated fiber show the important role of the hydride phase in the fracture of the fiber and the dispersion of the resulting powder. Hydrogenation of low-hydrogen alloys ($<0.65\% H$) results in a complete dissolution of hydrogen in the β and O phase lattices at this hydrogen content or possible precipitation of a small number of hydride particles which are not SEM- or XRD-visible. It does not lead to a sharp increase in the brittleness and a decrease in the ductility and can only initiate alloy fracture at lower stresses. This facilitates fiber fracture into long fragments and large particles in certain areas with a lower strength, possibly caused by an interplay of several factors: primary precipitation of discrete hydride particles, fiber surface defects, areas with thinner section, etc.

The destruction of orthorhombic alloys can be caused by the precipitation of the orthorhombic phase plates in the β phase matrix. It was shown [29] that during deformation of orthorhombic titanium aluminides the stresses induced in the β and O phases are quite different, with the O phase lamellar particles acting as stress concentrators contributing to the initiation and propagation of cracks in

the β -matrix of the alloy. As the number and size of the O phase plates increase, the difference in the stress between the β and O phases grows. SEM analysis of the microstructure of the rapidly solidified alloy containing 0.2% H shows that the thin O phase plates which precipitated during heating and holding at $800\ ^\circ C$ are uniformly distributed in the β phase grain body (Fig. 2b). An increase in the amount of introduced hydrogen leads to an increase in the number and distribution density of these plates in the β phase grains (Fig. 2d and f). However, they hardly affect the fracture of the fiber since a large number of O phase plates would initiate multiple cracks in the grain body and cause fiber destruction into small fragments, which we did not observe.

Alloy hydrogenation with higher concentrations (more than 1.0% H) results in partial or full transformation of the alloy from the highly hydrogenated state with the $\beta + O$ phase composition to a phase state which partially or completely consists of the intermetallic hydride which causes an increase in the volume stresses and rapid embrittlement of the alloy. It has a low ductility and a high hardness and destructs at low loads (Fig. 4). In this case, numerous cracks are initiated along the grain body or boundaries where destruction occurs during ball milling, and fine-dispersed alloy fragments (angular powders) can be produced.

The data on the effect of phase composition and hydrogen concentration on the fracture of the Ti_2AlNb -based alloy during ball milling show that to obtain HDH-powders, hydrogenation to a concentration of at least 1.0–1.2% is required at which the alloy has a high brittleness and fractures homogeneously into micro fragments (powders). Fine-dispersed HDH-powders are obtained by ball milling of the alloy hydrogenated with 1.5% H, and further increase in the hydrogen content has no visible effect on the dispersion of the powder. Hydrogenation of the Ti_2AlNb -based alloy with a concentration of 1.5% H can therefore be considered as the optimum parameter for the technology of HDH-powders. The synthesized powders of the intermetallic hydride have good cold compaction ability despite a high hardness and adhere mechanically due to the well-developed surface of the particles (Fig. 7).

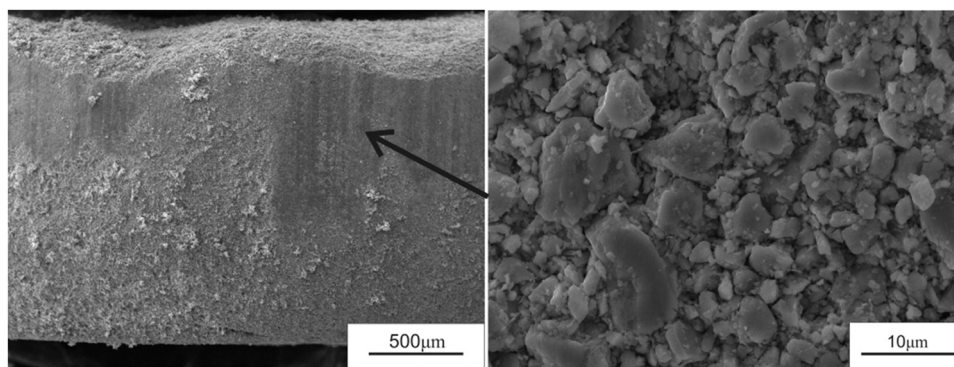


Fig. 7. End face of cold-compacted sample from the powder of intermetallic hydride containing 2.0% H.

5. Conclusions

The effect of hydrogen on the phase composition and microstructure of the rapidly solidified Ti₂AlNb-based alloy is studied. The effect of hydrogen content on the deformation of the rapidly solidified hydrogenated alloy during ball milling is determined. A high extent of powdering of the rapidly solidified alloy is achieved only by hydrogen alloying with 1.2 wt% H or higher when a transformation from a highly hydrogenated state into a hydride is observed in the alloy or the formation of a single hydride phase occurs. The possibility of producing fine-dispersed powders of the intermetallic hydride has been demonstrated for the Ti₂AlNb-based alloy.

Due to the well-suitable shape these pre-alloyed powders can be compacted at room temperature in contrast to the spherical atomized powders, thus they can be used to obtain orthorhombic titanium aluminides by cold compaction and pressureless sintering.

Funding

The study was carried out with a grant from the Russian Science Foundation (project No. 19-79-00327).

CRediT authorship contribution statement

K.S. Senkevich: Conceptualization, Methodology, Writing – original draft, Writing – review and editing, Supervision, Investigation. **O.Z. Pozhoga:** Writing – original draft, Funding acquisition, Project administration, Supervision, Investigation. **E.A. Kudryavtsev:** Investigation. **V.V. Zasyipkin:** Investigation.

Declaration of Competing Interest

The authors declare that they have no known competing financial interests or personal relationships that could have appeared to influence the work reported in this paper.

Acknowledgements

Authors express thanks to Serov M.M. for production of the rapidly solidified alloy by pendent drop melt extraction method.

TEM study was carried out on the equipment of the Center Collective Use "Materials Science and Metallurgy" NUST "MISIS".

References

- J. Kumpfert, Intermetallic alloys based on orthorhombic titanium aluminide, *Adv. Eng. Mater.* 3 (11) (2001) 851–864, [https://doi.org/10.1002/1527-2648\(200111\)3:11<851::AID-ADEM851>3.0.CO;2-G](https://doi.org/10.1002/1527-2648(200111)3:11<851::AID-ADEM851>3.0.CO;2-G)
- H. Zhang, N. Yan, H. Liang, Y. Liu, Phase transformation and microstructure control of Ti₂AlNb-based alloys: a review, *J. Mater. Sci. Technol.* 80 (2021) 203–216, <https://doi.org/10.1016/j.jmst.2020.11.022>
- M.C. Li, Q. Cai, Y.C. Liu, Z.Q. Ma, Z.M. Wang, Y. Huang, H.J. Li, Formation of fine B2/ beta plus O structure and enhancement of hardness in the aged Ti₂AlNb based alloys prepared by spark plasma sintering, *Metall. Mater. Trans. A* 48a (2017) 4365–4371, <https://doi.org/10.1007/s11661-017-4193-8>
- J. Jia, W. Liu, Y. Xu, C. Chen, Y. Yang, J. Luo, K. Zhang, B2 grain growth behavior of a Ti-22Al-25Nb alloy fabricated by hot pressing sintering, *J. Mater. Eng. Perform.* 27 (5) (2018) 2288–2297, <https://doi.org/10.1007/s11665-018-3353-3>
- Y.H. Zhou, W.P. Li, L. Zhang, S.Y. Zhou, X. Jia, D.W. Wang, M. Yan, Selective laser melting of Ti-22Al-25Nb intermetallic: significant effects of hatch distance on microstructural features and mechanical properties, *J. Mater. Process. Technol.* 276 (2020) 116398, <https://doi.org/10.1016/j.jmatprotec.2019.116398>
- I. Polozov, V. Sufiarov, A. Shamshurin, Synthesis of titanium orthorhombic alloy using binder jetting additive manufacturing, *Mater. Lett.* 243 (2019) 88–91, <https://doi.org/10.1016/j.matlet.2019.02.027>
- I. Polozov, V. Sufiarov, A. Kantyukov, A. Popovich, Selective laser melting of Ti₂AlNb-based intermetallic alloy using elemental powders: effect of process parameters and post-treatment on microstructure, composition, and properties, *Intermetallics* 112 (2019) 106554, <https://doi.org/10.1016/j.intermet.2019.106554>
- G. Wang, J. Yang, X. Jiao, Microstructure and mechanical properties of Ti-22Al-25Nb alloy fabricated by elemental powder metallurgy, *Mater. Sci. Eng. A* 654 (2016) 69–76, <https://doi.org/10.1016/j.msea.2015.12.037>
- D.P. Barbis, R.M. Gasior, G.P. Walker, J.A. Capone, T.S. Schaeffer, Titanium powders from the hydride-dehydride process, *Titan. Powder Met.* (2015) 101–105, <https://doi.org/10.1016/B978-0-12-800054-0.00007-1>
- M. Göknelma, D. Celik, O. Tazegul, H. Cimenoglu, B. Friedrich, Characteristics of Ti6Al4V powders recycled from turnings via the HDH technique, *Metals (Basel)* 8 (2018), p. 336, <https://doi.org/10.3390/met8050336>
- S. Abkowitz, S. Abkowitz, H. Fisher, Titanium alloy components manufacture from blended elemental powder and the qualification process, *Titan. Powder Met.* (2015) 299–312, <https://doi.org/10.1016/B978-0-12-800054-0.00017-4>
- O. Ivasishin, V. Moxson, Titanium powder metallurgy, low-cost titanium hydride powder metallurgy, *Titan. Powder Met.* (2015) 117–148, <https://doi.org/10.1016/B978-0-12-800054-0.00008-3>
- Z. Xu, B. Yuan, Y. Gao, Benefits in oxygen control and lowering sintering temperature by using hydride powders to sinter Ti-Nb-Zr SMAs, *J. Alloy Compd.* 838 (2020) 155572, <https://doi.org/10.1016/j.jallcom.2020.155572>
- V. Duz, M. Matviychuk, A. Klevtsov, V. Moxson, Industrial application of titanium hydride powder, *Met. Powder Rep.* 72 (2017) 30–38, <https://doi.org/10.1016/j.mprp.2016.02.051>
- T.-W. Na, K.B. Park, S.Y. Lee, S.-M. Yang, J.-W. Kang, T.W. Lee, J.M. Park, K. Park, H.-K. Park, Preparation of spherical TaNbHfZrTi high-entropy alloy powders by a hydrogenation-dehydrogenation reaction and thermal plasma treatment, *J. Alloy. Compd.* 817 (2020) 152757, <https://doi.org/10.1016/j.jallcom.2019.152757>
- S.Y. Lee, W.H. Lee, K.B. Park, S.H. Min, T.K. Ha, H.K. Park, Synthesis of Nb-Mo-Si based in situ composite powder by a hydrogenation-dehydrogenation reaction, *Mater. Lett.* 248 (2019) 32–35, <https://doi.org/10.1016/j.matlet.2019.03.134>
- K.C.G. Candioto, C.A. Nunes, Nb-20%Ta alloy powder by the hydriding-dehydriding technique, *Int. J. Refract. Met. Hard Mater.* 24 (6) (2006) 413–417, <https://doi.org/10.1016/j.ijrmhm.2005.06.001>
- K.S. Senkevich, O.Z. Umarova, V.V. Zasyipkin, Embrittlement of an orthorhombic Ti₂AlNb-based titanium alloy in a hydrogenated state, *Russ. Metall.* (2019) 31–35, <https://doi.org/10.1134/S0036029519010130>
- K.S. Senkevich, O.Z. Umarova, M.M. Serov, Obtainment of fibers and porous materials from Ti₂AlNb-based alloy, *Mater. Lett.* 203 (2017) 85–88, <https://doi.org/10.1016/j.matlet.2017.05.110>
- K.S. Senkevich, O.Z. Pozhoga, Experimental investigation of hydrogen absorption by commercial high alloyed Ti₂AlNb-based alloy in cast and rapidly solidified state, *Vacuum* 191 (2021) 110379, <https://doi.org/10.1016/j.vacuum.2021.110379>
- K.S. Senkevich, M.M. Serov, O.Z. Umarova, Fabrication of intermetallic titanium alloy based on Ti₂AlNb by rapid quenching of melt, *Met. Sci. Heat. Treat.* 59 (7–8) (2017) 463–466, <https://doi.org/10.1007/s11041-017-0172-3>
- L. Yang, M. Wang, B. Liul, Y. Du, W. Liao, In situ XRD study on the phase transformations of the gas-atomized Ti-22Al-25Nb powder, *Mater. Lett.* 277 (2020) 128378, <https://doi.org/10.1016/j.matlet.2020.128378>

- [23] S. Skvortsova, O. Pozhoga, V. Pozhoga, A. Ivanov, Effect of additional hydrogen alloying on the structure and the phase composition of a VTi-4 intermetallic alloy, *Russ. Metall.* (2019) 1151–1160, <https://doi.org/10.1134/S0036029519110107>
- [24] K. Ito, L.T. Zhang, V.K. Vasudevan, M. Yamaguchi, Multiphase and microstructure effects on the hydrogen absorption/desorption behavior of a Ti-22Al-27Nb alloy, *Acta Mater.* 49 (2001) 963–972, [https://doi.org/10.1016/S1359-6454\(00\)00402-X](https://doi.org/10.1016/S1359-6454(00)00402-X)
- [25] K. Ito, L.T. Zhang, V.K. Vasudevan, M. Yamaguchi, Hydrogen absorption/desorption behavior of Ti-22Al-27Nb alloys with β 0 single-phase and β /O two-phase microstructures, *Mater. Sci. Eng.* 329–331 (2002) 356–361, [https://doi.org/10.1016/S0921-5093\(01\)01600-8](https://doi.org/10.1016/S0921-5093(01)01600-8)
- [26] E. Tal-Gutelmacher, D. Eliezer, The hydrogen embrittlement of titanium-based alloys, *JOM* 57 (46–49) (2005), <https://doi.org/10.1007/s11837-005-0115-0>
- [27] X. Li, X. Ma, J. Zhang, E. Akiyama, Y. Wang, X. Song, Review of hydrogen embrittlement in metals: hydrogen diffusion, hydrogen characterization, hydrogen embrittlement mechanism and prevention, *Acta Metall. Sin. Engl. Lett.* 33 (2020) 759–773, <https://doi.org/10.1007/s40195-020-01039-7>
- [28] O.Z. Pozhoga, M.M. Serov, A.S. Yaroshenko, K.S. Senkevich, Study of mechanical properties of rapidly quenched fiber from orthorhombic alloy based on Ti₂AlNb, *J. Phys. Conf. Ser.* 1396 (1) (2019) 012033, <https://doi.org/10.1088/1742-6596/1396/1/012033>
- [29] Y. Fu, M. Lv, Q. Zhao, H. Zhang, Z. Cui, Investigation on the size and distribution effects of O phase on fracture properties of Ti₂AlNb superalloy by using image-based crystal plasticity modeling, *Mat. Sci. Eng.* 805 (2021) 140787, <https://doi.org/10.1016/j.msea.2021.140787>